HHS Public Access

Author manuscript

Ann Biomed Eng. Author manuscript; available in PMC 2016 October 01.

Published in final edited form as:

Ann Biomed Eng. 2015 October ; 43(10): 2552–2568. doi:10.1007/s10439-015-1301-z.

Umbilical Cord Blood-Derived Mononuclear Cells Exhibit Pericyte-Like Phenotype and Support Network Formation of Endothelial Progenitor Cells *In Vitro*

Erica B. Peters, **Betty Liu**, **Nicolas Christoforou**[*], **Jennifer L. West**, and **George A. Truskey**

Duke University, Durham, USA

[*]Biomedical Engineering Department, Khalifa University, P. O. Box 127788, Abu Dhabi, UAE

Abstract

Umbilical cord blood represents a promising cell source for pro-angiogenic therapies. The present study examined the potential of mononuclear cells (MNCs) from umbilical cord blood to support endothelial progenitor cell (EPC) microvessel formation. MNCs were isolated from the cord blood of 20 separate donors and selected for further characterization based upon their proliferation potential and morphological resemblance to human vascular pericytes (HVPs). MNCs were screened for their ability to support EPC network formation using an *in vitro* assay (Matrigel™) as well as a reductionist, coculture system consisting of no additional angiogenic cytokines beyond those present in serum. In less than 15% of the isolations, we identified a population of highly proliferative MNCs that phenotypically resembled HVPs as assessed by expression of PDGFR-β, NG2, α-SMA, and ephrin-B2. Within a Matrigel™ system, MNCs demonstrated pericyte-like function through colocalization to EPC networks and similar effects as HVPs upon total EPC tubule length ($p = 0.95$) and number of branch points ($p = 0.93$). In a reductionist coculture system, MNCs served as pro-angiogenic mural cells by supporting EPC network formation to a significantly greater extent than HVP cocultures, by day 14 of coculture, as evidenced through EPC total tubule length ($p < 0.0001$) and number of branch points ($p < 0.0001$). Our findings are significant as we demonstrate mural cell progenitors can be isolated from umbilical cord blood and develop culture conditions to support their use in microvascular tissue engineering applications.

Keywords

Angiogenesis; Vasculogenesis; Microvessel formation; Umbilical cord blood; Progenitor cells; Tissue engineering

Address correspondence to Erica B. Peters, Duke University, Durham, USA, ecb22@duke.edu.

Erica B. Peters and Betty Liu have contributed equally to this study.

Electronic Supplementary Material: The online version of this article (doi: 10.1007/s10439-015-1301-z) contains supplementary material, which is available to authorized users.

Introduction

Vascularization of tissue engineered-constructs remains an important goal for advancing the field of regenerative medicine.[34] Tissues developed *in vitro* are limited to a thickness of 150–200 μm due to the dependence on diffusion to meet oxygen and nutrient demands.[35,46] One solution to remove this size restriction placed upon scaffolds is to preform microvessel structures within the tissue-engineered constructs *in vitro*. Upon implantation, these microvessel structures could anastomose with the host vasculature, perfuse the construct, and enable function of the engineered tissue.

Current methods to engineer microvessel structures *in vitro* aim to recapitulate processes of both angiogenesis or vasculogenesis through coculture systems of the two vascular cell types required for stable microvessel formation: endothelial and mural cells.[1,15,37,39] During physiological microvessel formation, the release of angiogenic paracrine factors, such as vascular endothelial growth factor (VEGF), stimulates endothelial cells (ECs) from a quiescent state to an activated state.[1,9,18] The activated ECs degrade their basement membrane, proliferate, and arrange into lumenized microvessel structures. The ECs within these nascent capillary structures secrete cytokines, such as platelet-derived growth factor beta (PDGFB), that act to recruit mural cells, comprised of pericytes and vascular smooth muscle cells (SMCs).[1,9,18] These mural cells form tight associations with ECs,[1,9,18] functioning to stabilize the newly-formed capillaries by offering structural support, preserving the integrity of the EC permeability barrier, and providing cellular signals that prevent EC proliferation and apoptosis.

The choice of vascular progenitor cells is vital to the clinical translation of pre-vascularized tissues. The ideal progenitor cell source should enable isolation of both endothelial and mural progenitor cell types without requiring invasive surgery, be readily expandable *in vitro*, and carry a low risk of immunogenicity to the patient. Umbilical cord blood has the potential to meet these criteria due to its non-invasive isolation, capacity to undergo human leukocyte antigen (HLA) matching to improve immune tolerance, and potential to yield highly proliferative populations of vascular progenitor cells.[31,38,42] For example, cord blood derived-endothelial progenitor cells (EPCs) and mesenchymal progenitor cells (MPCs) can mimic the angiogenic role of mature endothelial cells and pericytes, respectively.[5,12,31,32,33,37] Specifically, cocultures of MPCs and EPCs embedded within a Matrigel™ matrix successfully generated microvessel structures *in vivo* as demonstrated through anastomosis to host vasculature that remained functional for 4 weeks.[31]

In order to utilize MPCs and EPCs for angiogenic therapies, however, there remains a need to clearly define their isolation and characterization methods. While isolation and characterization procedures for obtaining angiogenic EPCs are well defined and largely consistent among groups,[19,21,29,45] there exist several methodologies for isolating MPCs that vary by the mononuclear cell (MNC) isolation technique, expansion medium, and substrate coating.[25,26,47] The most common method for MPC isolation utilizes density gradient centrifugation of cord blood to isolate MNCs with the subsequent selection of MPCs based upon their adherence to uncoated tissue-culture plastic.[12,26,38] Derivation of MPCs can also occur through inducing endothelial-to-mesenchymal transition

(EndMT).[26,30,33] In this approach, EPCs are first derived from MNCs before treatment with transforming growth factor-beta proteins. The MPCs resulting from EndMT procedures exhibit a contractile, SMC phenotype with pro-angiogenic paracrine properties.[33] In addition, isolation methods employing EndMT have demonstrated success rates near 100% for achieving MPCs,[26,30,33] an improvement over traditional isolation methods success rates which vary from 10 to 60%.[25,26,47]

Regardless of the isolation technique chosen to derive MPCs, there exists heterogeneity in the resulting MPC populations. For example, two distinct populations of MPCs, characterized as flattened or spindle-shaped morphology, can arise from MNCs and demonstrate variances in growth kinetics and differentiation capacity.[28] This observation, combined with recent reports demonstrating that not all MSCs exhibit pericyte function,[7,10] make evident the need to functionally characterize the pericyte-potential of MPCs to ensure successful translation into angiogenic therapies. In this study, we sought to define a population of mural progenitor cells arising from cord blood MNCs that could support robust, network formation of EPCs. Our criteria for defining mural progenitor cells included: (1) spindle-shaped population with phenotypic similarity to human vascular pericytes (HVP) through expression of pericyte-associated markers alpha-smooth muscle actin (α-SMA), PDGFR-β, chondroitin sulfate proteoglycan 4 (NG2) and ephrin-B2[2,3,17] (2) a highly proliferative population demonstrating a minimum tenfold increase in cell yield from primary culture over 8 weeks of *in vitro* expansion (3) perivascular localization to, and support of, EPC networks evaluated through *in vitro* angiogenesis assays.

Materials and Methods

Isolation of MPCs and EPCs

To investigate the hypothesis that mesenchymal progenitor cells (MPCs) morphologically resembling pericytes could be derived from umbilical cord blood, we employed two isolation techniques commonly used to isolate MPCs, denoted as the traditional method[26] (TM) and endothelial-to-mesenchymal transition method[30] (EndMT). Umbilical cord blood from 20 separate biological donors was obtained through the Carolina Cord Blood Bank following procedures approved by the Duke University Institutional Review Board. Cord blood was diluted with Hank's Balanced Salt Solution (HBSS) (Gibco®, Life Technologies, Carlsbad, CA, USA) at a 1:1 ratio and carefully layered atop Histopaque-1077 (Sigma-Aldrich, St. Louis, MO, USA) solution. The resulting blood/HBSS mixture was separated into erythrocyte, MNC, and plasma layers through centrifugation at 740 g. The traditional method of MPC isolation[26] consisted of plating MNCs onto T-75 flasks supplemented with Iscove's Modified Dulbecco's Medium (IMDM) (Sigma-Aldrich) containing 10 ng/ml fibroblastic growth factor-basic (R&D systems, Minneapolis, MN, USA), 2 mM L-glutamine (Lonza, Walkersville, MD, USA), 20% v/v fetal bovine serum (FBS) (Atlanta Biologics, Law-renceville, GA, USA), and 1% v/v penicillin streptomycin solution (Corning, Corning, NY, USA). After 30 days of culture, adherent MNCs were passaged using 0.25% trypsin–EDTA (Gibco®) and expanded at 1.33×10^4 cells/cm^2.

In contrast, the EndMT method first required the isolation of EPCs. EPCs were isolated as previously described.[21] MNCs were plated onto 6-well polystyrene plates, pre-coated for 1 h

with 50 μg/mL of collagen I (BD Biosciences, San Jose, CA, USA), and supplemented with complete endothelial growth media (EBM2 with EGM2 bullet kit), a total of 50 mL (8.9% v/v) of FBS, and 5 mL (0.9% v/v) of penicillin streptomycin solution. To obtain MPCs using the EndMT method,[33] confluent, primary passage EPCs were treated with RPMI 1640 media (Sigma-Aldrich) supplemented with 20% v/v FBS, 2 mM L-glutamine, and 10 ng/mL of TGF-β2 (R&D systems). After 21 days of treatment, the media was changed to RPMI 1640 media (Sigma-Aldrich) supplemented with 20% v/v FBS and 2 mM L-glutamine. EndMT-derived MNCs were passaged using 0.25% trypsin–EDTA and expanded at 1.33×10^4 cells/cm^2.

To obtain EPCs for angiogenesis coculture assays, adherent MNCs displaying cobblestone-like EC morphology were passaged by 22 days, after initial MNC plating using the EPC method, with 0.025% trypsin– EDTA and confirmed for EPC phenotype through flow cytometry analysis and immunofluorescence. Endothelial outgrowth cells from EPCs were expanded at 6.67×10^3 cells/cm^2 with endothelial growth media. MNCs morphologically resembling pericytes from three separate donors were used between passages 3–5 for all experiments. EPCs derived from three separate donors were used between passages 3–6 for all experiments. The population doubling time (PDT) for MNCs was determined by the following formula:

$$\begin{gathered}\mathrm{PDT}=\mathrm{Time\ interval\ between\ cell\ seeding\ and\ harvest}/\mathrm{PD} \\ \mathrm{PD}=\mathrm{population\ doubling}=\log \mathrm{CH}/\mathrm{CS} \\ (\mathrm{CH}=\mathrm{cell\ number\ at\ harvest}, \mathrm{CS}=\mathrm{cell\ number\ at\ seeding})\end{gathered}$$

Cell Culture

In order to characterize the pericyte potential of MNCs, human brain vascular pericytes (HVPs) (ScienCell, Carlsbad, CA, USA) were cultured in medium containing 10 mL of FBS, 5 mL of pericyte growth supplement, and 5 mL of penicillin/streptomycin solution (ScienCell). Pericytes were seeded at 1.33×10^4 cells/cm^2 on tissue-culture plastic, precoated for 1 h with 2 μg/cm^2 poly-L-lysine (Sigma). HVPs were used between passages 5–8 for all experiments. Human umbilical vein-derived endothelial cells (HUVECs) from pooled donors (Lonza) were used as an EC reference to characterize EPCs. HUVECs were expanded in the same endothelial growth medium as EPCs with a total FBS concentration of 2% v/v and used between passages 3-6 for all experiments. To further evaluate the mural cell potential of MNCs, we utilized human aortic vascular smooth muscle cells (SMCs) (Lonza) cultured in smooth muscle basal medium supplemented with smooth muscle growth media-2 SingleQuots (Lonza) and 1% v/v penicillin streptomycin solution. SMCs were used between passages 6–8 for all experiments.

Characterization of MNCs for Mesenchymal and Endothelial Gene Expression

We employed quantitative real-time polymerase chain reaction (qRT-PCR) methods to assess the expression of genes associated with mesenchymal stem cells (alpha smooth muscle actin/α-SMA, fibroblast-specific protein 1/FSP-1) and endothelial cells (vascular endothelial cadherin/VE-cadherin, platelet endothelial cell adhesion molecule/PECAM-1)

(Table 1).[30] A two-step cycle configuration was performed with an initial denaturation for 3 min at 95°C and 50 cycles at 95°C for 15 s and 61°C for 1 min. All samples were performed in triplicate for all genes. The 2 (–Delta Delta *C*(*T*)) method was used to determine relative gene expression to SMCs. The housekeeping gene was 18 s rRNA.

Surface Antigen Characterization of MNCs

To evaluate the mesenchymal phenotype of SS-MNCs, we performed flow cytometry analysis using a BD FACSCalibur™ cell analyzer (BD Biosciences) for the expression of mesenchymal lineage-associated surface antigens CD105, CD73, CD90 and lack of expression for hematopoietic lineage-associated surface antigens CD45, CD34, HLA-DR, CD19, and CD14 (Biolegend, San Diego, CA, USA). IgG mouse isotype (Biolegend) served as a negative control. FITC-conjugated antibodies were added to SS-MNCs at a concentration of 2 μL/10^5 cells.

To confirm EC phenotype of EPCs derived from MNCs, EPCs at passage 3 were analyzed with flow cytometry for expression of EC-associated markers CD31, CD146, CD105, CD309/VEGFR2; expression of hematopoietic progenitor cell markers CD34, CD133; lack of expression for leukocyte markers CD45, CD14, and the MSC/fibroblast-associated marker CD90. Pre-conjugated antibodies to FITC or PE (Biolegend) were added at a concentration of 2 μL/10^5 cells. CD133 (Miltenyl Biotec, San Diego, CA, USA) was used at a concentration of 10 μL/10^5 cells. HU-VECs served as an EC control. IgG mouse isotype conjugated to FITC or IgG goat isotype conjugated to PE (Biolegend) served as negative controls. A minimum of 9000 gated events were analyzed per condition.

Differentiation of SS-MNCs Towards Adipogenic, Osteogenic, and Chondrogenic Lineages

In order to evaluate mesenchymal function of the SS-MNCs, we assessed their ability to differentiate towards adipogenic, osteogenic, and chondrogenic lineages with StemPro® differentiation kits (Invitrogen™, Life Technologies, Carslbad, CA, USA). Following the manufacturer's suggestions, SS-MNCs were cultured in osteogenic, adipogenic, or chondrogenic induction media for 24, 10, and 15 days, respectively. At the end of induction, cultures were rinsed twice with Dulbecco's Phosphate Buffered Saline (PBS), without calcium chloride and magnesium chloride (Sigma-Aldrich) and preserved through the addition of 10% formalin for 1 h.

Alizarin Red (Sigma-Aldrich) staining was used to indicate osteoblast mineralized matrix. Oil Red O staining (Sigma-Aldrich) was employed to visualize lipid vacuole formation. To demonstrate chondrogenic differentiation of SS-MNCs, Alcian blue (Sigma-Aldrich) was used to stain for the presence of proteoglycans. Alcian blue was prepared at a 1% concentration in 0.1 N HCl and added to preserved samples for 30 min before rinsing with distilled water. The resulting samples were imaged with a Nikon® Eclipse Inverted Microscope system (Nikon Instruments Inc. Americas, Melville, NY, USA).

Immunofluorescence to Evaluate Pericyte Phenotype of SS-MNCs

To evaluate the potential pericyte phenotype of the SS-MNCs, we performed immunofluorescence to detect expression of PDGFR-β, α-SMA, NG2, and ephrin-B2. To

confirm the SS-MNCs as a population separate from EPCs, we examined the SS-MNCs for expression of VE-cadherin. EPCs were further characterized for expression of EC functional proteins endothelial nitric oxide synthase (eNOS) and von Willebrand Factor (vWF). Cultures of SS-MNCs, HVPs, or EPCs were plated on 8-well chamber slides (Nunc™ Lab-Tek™ II Chamber Slide™, Thermo Fisher Scientific, Rochester, NY, USA) and allowed to reach confluency prior to fixation with 4% paraformaldehyde for 10 min.

To prevent non-specific binding, cultures were incubated overnight at 4°C with 3.5% bovine serum albumin (BSA) (Thermo Fisher Scientific). Primary antibodies of PDGFR-β (2 μg/mL, Santa Cruz Biotechnology, sc-432, Santa Cruz, CA, USA), α-SMA (2 μg/mL, Abcam, ab7817, Cambridge, MA, USA), NG2 (6 μg/mL, Abcam, ab83178), ephrin-B2 (10 μg/mL, Abcam, ab131536) VE-cadherin (2 μg/mL, Santa Cruz Biotechnology, sc-6458), eNOS (2 μg/mL, Santa Cruz Biotechnology, sc-654), vWF (2 μg/mL, Santa Cruz Biotechnology, sc-53466) were diluted with BSA and added to preserved cultures for overnight incubation at 4°C. To prevent non-specific secondary antibody binding, cultures were rinsed twice with PBS containing 0.01% Tween®20 (Sigma-Aldrich) and once with PBS prior to adding secondary antibodies (donkey anti-mouse/donkey anti-rabbit/donkey anti-goat AlexaFluor 488 and donkey anti-rabbit AlexaFluor 555, Invitrogen™) diluted 1:200 in BSA for overnight incubation at 4°C. To observe nuclei, cells were incubated with 4,6-diamidino-2-phenylindole (DAPI) (Molecular Probes®, Life Technologies) for 2 h before rinsing twice with PBS.

An inverted confocal microscope (Leica DMI6000CS, Leica Microsystems Inc., Buffalo Grove, IL, USA) captured immunofluorescence images with a 40× oil-immersion objective. To avoid spectral bleed-through, we performed sequential scanning with separate channels for excitation of the 405, 488, and 561 nm lasers. Four images were taken per condition at a depth of 12 μm, compiled from 2 μm slices, using 1024 × 1024 pixels, and a line and frame average of 2. Images were reconstructed with Imaris software (Bitplane USA, South Windsor, CT, USA). To quantitatively compare the intensity of protein expression between SS-MNCs, HVPs and EPCs, integrated pixel measurements were taken on immunofluorescence images with FIJI software and normalized to cell number per image.

Matrigel™ In Vitro Angiogenesis Assay to Evaluate the Pericyte Function of SS-MNCs

Matrigel™ (Corning) was coated upon tissue-culture treated μ-slides designed for investigating angiogenesis (ibidi, Verona, WI, USA) at 10 μl per well, resulting in an 800 μm-thick gel. To visualize network structures, SS-MNCs, HVPs, HUVECs, and EPCs were transduced with either green fluorescent protein (GFP) or tdTomato red fluorescent protein using a previously established protocol.[5] Monoculture controls of each cell type were plated at 1×10^4 cells/well. Cocultures of SS-MNCs and HVPs with either HUVECs or EPCs were plated at a 1:1 ratio using the same total cell number as the monoculture conditions. Cultures were supplemented with EBM2 media containing 2% v/v FBS and 1% v/v penicillin streptomycin solution. After 6 h of culture, samples were preserved with 4% paraformaldehyde for 10 min. Network formation was captured through confocal imaging (Leica) using a 10× objective with an image depth of 200 μm compiled from 10 μm sections. Network images were reconstructed with Imaris software and analyzed for total tubule

length and number of branch points using Metamorph® Angiogenesis Tube Formation Application (Molecular Devices, Sunnyvale, CA, USA). The minimum and maximum widths for defining tubules were 13 and 84 μm, respectively.

Coculture In Vitro Angiogenesis Assay to Evaluate the Pericyte Function of SS-MNCs

To assess whether SS-MNCs could form perivascular associations under conditions that mimicked physiological microvessel formation, we utilized a previously established *in vitro* angiogenesis assay composed of angiogenic mural cells (SMCs) mixed with EPCs upon uncoated tissue culture plastic at seeding numbers of 8×10^4 cells/cm^2 and 4.8×10^4 cells/cm^2, respectively[37]. SS-MNCs were added to EPCs and SMCs at ratios varying from 1:16:4 to 1:0.1:4 EPC to SS-MNCs to SMCs. The total number of SS-MNCs and SMCs was maintained at 8×10^4 cells/cm^2 and EPC numbers were kept constant at 4.8×10^4 cells/cm^2 for all ratios of SS-MNCs. These tri-cultures were plated upon 24-well tissue-culture plastic plates (Corning) and maintained in EBM2 media containing 9% v/v of FBS, and 0.9% v/v of penicillin streptomycin solution. After 9 days of culture, images were taken of SS-MNCs (transduced with GFP) and EPCs (transduced with tdTomato) using a Nikon® Eclipse Inverted Microscope system. EPC networks were quantified using Metamorph's Angiogenesis Tube Formation module using the same parameters as the Matrigel™ assay analysis. To evaluate the effect of SS-MNCs on the tortuosity of EPC networks, we measured the angle of curvature between adjacent EPC segments that comprised a branch point using ImageJ software.

SS-MNCs were also investigated for their ability to support EPC networks upon coculture in comparison to SMCs and HVPs. EPCs were mixed with SS-MNCs, SMCs, or HVPs at a 1:4 ratio for a total cell number of 1.28×10^5 cells/cm^2 on 24-well tissue-culture plastic plates (Corning) and maintained in EBM2 media containing 9% v/v of FBS, and 0.9% v/v of penicillin streptomycin solution. Images of tdTomato-transduced EPCs were taken during the first 14 days of coculture using a Nikon® Eclipse Inverted Microscope system. To evaluate whether media conditions could enhance the rate of EPC network formation in SS-MNC cocultures, osteogenic media conditions were used in place of EBM2 media conditions.[36] Osteogenic media (STEMCELL™ Technologies, Vancouver, BC, Canada) consisted of MSC basal medium containing an osteogenic stimulatory supplement, 1 M β-glycerophosphate, 1 mg dexamethasone, and 100 mg ascorbic acid. EPC monocultures (4.8×10^4 cells/cm) supplemented with osteogenic media were used as a control. Images of the resulting EPC microvascular structures were taken with an inverted confocal microscope (Leica) at a depth of 100 μm with 2 μm slices.

Statistical Analysis

To investigate statistical significance between conditions, we used one or two-factor analysis of variance (ANOVA) followed by a *post hoc* Tukey honest significant difference test for multiple comparisons using the JMP® statistical software platform (SAS, Cary, NC, USA).

Results

A Spindle-Shaped Subpopulation of Mononuclear Cells (SS-MNCs) Derived from Umbilical Cord Blood Morphologically Resemble Pericytes

We observed MNCs with distinct morphologies arising from each isolation method (Fig. 1a). The EPC method yielded MNCs exhibiting a cobblestone morphology. In contrast, fibroblast-like cells were observed with TM techniques. EndMT methods yielded cells exhibiting a mix of phenotypes seen in both EPC and TM isolations. Interestingly, in all of the isolation methods, we discovered a subpopulation of MNCs, described as spindle-shaped MNCs (SS-MNCs), which bore a striking resemblance to HVP shown by morphological comparisons at subconfluent and confluent conditions (Figs. 1a and 1b). These SS-MNCs were not dependent on the isolation method nor individual donors. For instance, SS-MNCs obtained using EPC isolation methods were not consistently observed in the TM and EndMT isolations that were performed in parallel using the same donor. Further, the EPC method resulted in slightly higher isolation success rates, near 15%, in comparison to the 10% isolation success rate observed with TM and EndMT methods. While treatment of MNCs with TGF-β2 during primary passage (EndMT method) to induce the EndMT process did not result in significant increases in SS-MNCs, increases of gene expression for mesenchymal-associated markers α-SMA and fibroblast-specific protein 1 (FSP-1), and corresponding decreases in endothelial cell markers VE-cadherin ($p < 0.002$) and PECAM-1 were observed in TGF-β2-treated MNCs in comparison to untreated MNCs (Supplemental Fig. 1).

The SS-MNCs derived from the EPC isolation method contained the greatest expansion potential in comparison to SS-MNCs isolated by the TM and EndMT methods, as demonstrated by a tenfold increase in cell number to over 10 million cells after 8 weeks of culture (Fig. 1c). This result indicates the media composition affects the proliferative potential of SS-MNCs with endothelial growth media favorable for expansion over basal media conditions. The average population doubling time for SS-MNCs using the EPC method was 21 ± 5 days (Fig. 1d), which was not significantly different ($p = 0.11$) from the doubling time for the traditional method (47 ± 20 days) or the EndMT method (40 ± 2 days) over a culture period of 45 days.

To examine the extent of pericyte phenotype displayed by the SS-MNCs derived from EPC isolation methods, we performed immunostaining for the following panel of markers expressed by pericytes: PDGFR-β, α-SMA, NG2, and ephrin-B2.[2,3,17] Due to the use of endothelial cell isolation techniques and growth medium for the expansion of SS-MNCs, we sought to demonstrate the unique phenotype of SS-MNCs through immunostaining for VE-cadherin and corresponding immunostaining for pericyte markers on EPCs. Approximately 100% of the SS-MNCs expressed PDGFR-β, α-SMA, and NG2 (Fig. 2a). VE-cadherin was also expressed in up to 17% of the total SS-MNC population. We observed similar expression for PDGFR-β ($p = 0.27$) and α-SMA ($p = 0.56$) between SS-MNCs and HVPs based on the intensity of fluorescence, evaluated through the integrated pixel density per cell (Fig. 2b). SS-MNCs contained significantly lower levels of NG2 expression ($p = 0.006$) and higher levels of ephrin-B2 ($p = 0.02$) and VE-cadherin ($p = 0.007$) than HVPs.

Although the fluorescence intensity of VE-cadherin in SS-MNCs did not significantly differ from EPCs ($p = 0.18$), the pattern of expression was diffuse in contrast to distinct localization within adjacent cell– cell contacts seen in EPCs (Fig. 2a). HVPs lacked observable VE-cadherin expression. The EPCs contained significantly lower levels of PDGFR-β ($p = 0.018$), NG2 ($p = 0.005$), and ephrin-B2 ($p = 0.004$) expression in comparison to SS-MNCs. As well, EPC expression for PDGFR-β, NG2, and ephrin-B2 was localized near the nucleus, in contrast to the membrane-localized expression patterns observed in HVPs and SS-MNCs. Further characterization of EPCs supported their EC phenotype based on expression of vWF and eNOS. In addition, flow cytometry analysis demonstrated the majority of the EPC population expressed EC markers CD31 (92.1%), CD146 (95.9%), CD105 (99.9%), and as well as expression for CD309/VEGFR2 (35.8%). In addition, EPCs contained higher amounts of the hematopoietic stem cell marker CD34 (16.9%) in comparison to HUVECs (3.9%); and lack ofexpression (<0.1%) for the leukocyte markers CD45, CD14, and the fibroblast/MSC-associated marker CD90. (Supplemental Figs. 2, 3). Therefore, despite the use of EPC isolation techniques, the SS-MNCs are distinct from EPCs based on their expression for pericyte-associated proteins PDGFR-β, NG2, and ephrin-B2.

SS-MNCs Contain Functional Properties of Mesenchymal Stem Cells and Pericytes

In order to clarify the identity of the spindle-shaped MNCs, we analyzed cell markers and functions associated with mesenchymal stem cell (MSC) and pericyte phenotypes. The minimum standards for defining MSCs[14] include: (1) adherence to plastic (2) surface antigen expression positive (>95%) for CD105, CD73, CD90, and negative (<2%) for CD45, CD34, HLA-DR, CD19, CD14 and (3) *in vitro* differentiation towards osteoblasts, adipocytes, and chondroblasts demonstrated through von Kossa, Oil Red O, and Alcian blue staining, respectively. SS-MNCs could adhere to plastic and were expanded in uncoated tissue-culture flasks. SS-MNCs showed positive expression (>98%) for CD73, partial expression for CD105 (27%) and CD90 (14.5%), and lack of expression (< 1%) for CD45, CD34, HLA-DR, CD19, and CD14 (Fig. 3a). To assess their differentiation potential, we cultured SS-MNCs with media formulated for the induction of MSCs towards adipogenic, chondrogenic, and osteogenic media. Although the SS-MNCs lacked adipogenic differentiation potential, shown by the absence of lipid vacuole formation indicated by Oil Red O staining, they were shown to differentiate into osteoblasts and chondroblasts through positive von Kossa staining for mineralized matrix and Alcian blue staining for the presence of proteoglycans (Fig. 3b). Therefore, the SS-MNCs, while demonstrating mesenchymal-like function through differentiation towards osteogenic and chondrogenic lineages, are not MSCs as defined by the International Society for Stem Cell Research[12] due to their lack of adipogenic differentiation and surface antigen expression for CD90 and CD105.

To determine whether the SS-MNCs exhibit pericyte function, we employed the use of a Matrigel™ *in vitro* assay.[11] After 6 h of plating, SS-MNCs colocalized to EC networks in a similar manner as HVPs, at depths up to 100 μm from the gel surface (Fig. 4a). Specifically, SS-MNCs demonstrated perivascular localization to HUVEC networks in the same manner as HVPs and had no significant differences upon HUVEC total tubule length ($p = 0.85$) and number of branch points ($p = 0.96$) (Figs. 4b and 4c). To further support the use of cord

blood as a single cell source for angiogenesis-based therapies, we also evaluated the network formation potential of EPCs in comparison to HUVECs. EPCs showed significantly ($p < 0.0001$) higher network formation potential than HUVECs based on a threefold increase in total tubule length and near fourfold increase in number of branch points (Figs. 4b and 4c). While we observed a decrease in EPC total tubule length and number of branch points in SS-MNC cocultures, these inhibitory effects upon EPC network formation were also observed with HVPs, as shown through a lack of significant differences between EPC total tubule length ($p = 0.95$) and number of branch points ($p = 0.93$). In addition, co-cultures of EPCs and SS-MNCs were able to form network structures to the same extent as cocultures of mature endothelial cells (HUVECs) and pericytes (HVPs) based on similar values for EC total tubule length ($p = 0.98$) and number of branch points ($p = 0.99$).

Taken together with the MSC and pericyte characterization results, these observations suggest SS-MNCs represent a distinct population of vascular progenitor cells that contains functional properties of both MSCs and HVPs.

In the Absence of Biologically-Derived Matrix Substrates and Supplemental Growth Factors, SS-MNCs, When Combined with SMCs at Low Ratios, Demonstrate Perivascular Localization to EPC Networks

While Matrigel™ substrates provide a useful screening assay to assess the angiogenic potential of progenitor cells, insights gained from these results were limited to 24 h of observation, after which we saw regression of EC networks. As well, the Matrigel™ matrix is derived from tumor-basement membrane,[22] promoting potential cancer-like vessels. Therefore, to further examine the effect of SS-MNCs on EPC network formation, we combined SS-MNCs in a tri-culture system with EPCs and SMCs. The SMCs can replace the use of biologically-derived matrix substrates to support robust, stable microvessel formation of EPCs that closely mimics physiological processes of microvessel formation seen *in vivo*.[23,37,39]

SS-MNCs added simultaneously to EPCs and SMCs, and examined 9 days after formation of tri-cultures, inhibited vessel formation in a concentration-dependent manner, as evidenced through a decrease in the number of branch points, average segment length, and angle of curvature (Figs. 5a–5c). Tri-cultures containing low amounts of SS-MNCs (below 1:4:4 EPC:SS-MNC:SMC) enabled the formation of EPC networks that contained perivascular localized SS-MNCs. HVPs demonstrated similar perivascular-like localization to EPC networks as SS-MNCs at a low HVP: SMC ratio (Supplemental Fig. 4). A tenfold reduction in SS-MNC, from 1:1:4 to 1:0.1:4 EPC:SS-MNC:SMC, resulted in extensive connectivity of EPC networks shown by a threefold increase in the number of branch points (Figs. 5b and 5c). These observations indicate SS-MNCs, when placed in tri-culture with SMCs and EPCs, may secrete inhibitory factors that prevent EC network formation. The presence of SMCs, at several fold higher ratios than SS-MNCs, counteracts this inhibitory effect of SS-MNCs on EPC network formation without affecting the ability of SS-MNCs to interact with EPC networks in a pericyte-like manner.

SS-MNCs Contain the Potential to Serve as an Angiogenic, Mural Cell Source for the In Vitro Formation of EPC Networks

During vascular development, ECs secrete PDGF, recruiting mesenchymal precursor cells to stabilize the developing microvessel structure.[43] Once contact is established between ECs and MSCs, latent TGF-β1 is released, resulting in differentiation of MSCs towards a mural cell phenotype that can support microvessel formation by EPCs.[16] Although the SS-MNCs express mural cell markers, NG2, PDGFR-β, α-SMA, and ephrin-B2; extended coculture with EPCs may provide the necessary microenvironmental cues to elicit their pro-angiogenic function. To test this hypothesis, we examined the effect of SS-MNCs upon EPC network formation for 2 weeks under coculture *in vitro* conditions that did not contain supplemental growth factors, biologically-derived matrix, or additional angiogenic mural cells. We compared our findings to EPCs in coculture with mural cell types of SMCs or HVPs. SS-MNCs appeared to inhibit EPC network formation for the first 6 days of culture, when compared to SMC cocultures, as evidenced through the presence of EPC clusters that did not elongate to form capillary-like networks (Figs. 6a and 6b). EPCs in coculture with HVPs showed similar morphology to SS-MNC cocultures. However, by day 10 of culture, the clusters of EPCs present in SS-MNC conditions developed highly connected, mesh-like structures of networks not observed with HVP cocultures.

Overlay images of EPCs in cocultures of SMCs, SS-MNCs, or HVPs revealed homogeneous distribution of SMCs and SS-MNCs in contrast to HVPs which were localized adjacent to EPCs (Fig. 6c). By day 14 of culture, SS-MNC coculture conditions demonstrated a significantly higher number of branch points ($p < 0.0001$) and increased total tubule length ($p < 0.0001$) than HVP coculture conditions. The EPC networks formed in coculture with SS-MNCs persisted for at least 18 days (Supplemental Fig. 5). We conclude from these observations that SS-MNCs have the potential to act as an angiogenic mural cell source to support network formation by EPCs.

EPC Network Formation in SS-MNC Cocultures Can Occur Under Osteogenic Media Conditions

While SS-MNCs supported network formation of EPCs, network structures took nearly twice as long to develop with SS-MC cocultures than with SMC cocultures. The substitution of osteogenic media, in place of basal media conditions, enhances the ability of mesenchymal progenitor cells to support EC network formation by increasing the total tubule length within 6 days of coculture.[36] We hypothesized the addition of osteogenic media could also enhance the rate of EPC network formation in SS-MNC cocultures in comparison to basal media conditions, which contain no additional growth factors beyond those present in serum.

To test our hypothesis, we repeated coculture experiments of SS-MNC and EPCs using osteogenic media conditions, which contained, in addition to serum, dexamethasone, β-glycerophosphatase, and ascorbic acid. We observed no increase in the onset of network formation with SS-MNC and EPC cocultures containing osteogenic media (Fig. 7a) in comparison to coculture conditions containing basal media with serum (Fig. 6a). However, the EPCs in osteogenic media conditions formed 3D nodules containing microvasculature

structures (Figs. 7a–7c). The SS-MNCs both surrounded and incorporated into the 3D nodules, where they appeared to function as a matrix support to the 3D EPC microvessel structures (Fig. 7b). Therefore, while the use of osteogenic media does not enhance the rate of EPC network formation in SS-MNCs cocultures, it causes the formation of 3D vascularized nodules not seen in EPC monocultures or EPC and SS-MNC cocultures utilizing basal media.

Discussion

In this study, we isolated a population of spindle-shaped MNCs from human umbilical cord blood that phenotypically resemble pericytes based on their expression of PDGFR-β, α-SMA, ephrin-B2, NG2, and perivascular localization to EC network structures. Further, these SS-MNCs possessed angiogenic mural cell function, shown through their ability to support network formation of EPCs under coculture conditions containing minimal angiogenic stimulants. Interestingly, we found osteogenic media conditions stimulated the development of 3D vascularized-nodules of EPCs in SS-MNC cocultures.

Increasing the isolation success rate and purity of mesenchymal cells from tissues is a major focus for regenerative medicine.[41] Isolation of MSCs from umbilical cord blood as an allogenic cell source is of interest due to their availability and ease of procurement. Recently, groups have reported methods to improve the purity of MSCs by using surface antigens.[4,20] While this approach can yield pure populations of MSCs, the time and cell doubling rate required to reach therapeutically-relevant cell numbers can lead to senescent cells that no longer possess angiogenic characteristics of MSCs observed at earlier passages.[13,24,44] In this work, we found a highly proliferative population of MNCs from cord blood morphologically resembling pericytes was possible. The lack of difference in isolation success rates between TM and EndMT methods was surprising, considering the previously reported successes of the EndMT method.[26,30,31] A reason for the discrepencies between reported SS-MNC isolation success rates from those found in our study may be due to our requirements for isolation success which includes the SS-MNCs obtained from a single donor to expand in cell numbers of over 10 million cells by 8 weeks of culture. Surprisingly, we found pre-coating with collagen I and the use of EGM2 growth factors utilized in EPC isolation techniques not only supported SS-MNC attachment but also resulted in rapid cell expansion to over 10 million cells in a period of 8 weeks. One explanation for this effect is that the presence of growth factors within EGM2-containing media, such as VEGF and FGF2, simulate an angiogenic microenvironment that stimulates both EPC and pericyte growth.[1,3,18] Further investigations are needed to support this hypothesis as well as to optimize the media conditions for the isolation and expansion of SS-MNCs.

Although the SS-MNCs did not meet the minimum criteria to be defined as MSCs,[14] they demonstrated near 100% expression of pericyte markers PDGFR-β, NG2, α-SMA. The SS-MNCs also exhibited diffuse VE-cadherin expression, indicating the possibility of an EPC origin. The heterogeneous expression of SS-MNCs in our study for both SMC-like (α-SMA) and fibroblast-associated (CD90) markers may indicate the potential for fibroblast differentiation, impacting their end-use as pericytes in tissue-specific applications such as

myogenesis.[6] Therefore, characterization of MSC-like cells for pericyte and fibroblast-associated markers, in addition to *in vitro* angiogenesis assays assessing their ability to function as mural cells, may be the best approach for the selection of these cells in angiogenic therapies.

As well, more stringent assays are needed to identify SS-MNCs as true “mural progenitors”, such as those previously employed to define EPCs.[21] For example, single cell proliferation assays and clonogenic capacity, as well as the ability of SS-MNCs to integrate and function alongside mural cells *in vivo*, will help support their mural progenitor cell identity.

While our Matrigel™ assay results indicated a greater sensitivity of EPCs to the addition of SS-MNCs than HUVECs, there was no significant difference in the resulting total tubule length and number of branch points in comparison to HUVEC and SS-MNC cocultures. Inhibitory factors secreted by SS-MNCs to prevent further EPC network formation is consistent with the physiological function of pericytes to stabilize nascent microvessel structures.[1,2] The Matrigel™ matrix is also limited in its ability to offer thorough analysis of SS-MNC pericyte function due to the lack of EC network stability we observed after 24 h. The immature SS-MNCs may require additional time to differentiate towards a pro-angiogenic mural cell type, which we observed by 2 weeks of coculture with EPCs based on the support of EPC network formation (Fig. 6).

Interestingly, the patterns of EPC clusters observed upon coculture with SS-MNC, and their subsequent development into a mesh-like structure of microvascular networks by day 10 of coculture, resembles patterns of EPCs observed during vasculogenesis where aggregates of EPCs form blood islands that fuse to form primary capillary plexus.[1,18] *In vivo*, the development of capillary sprouts from vascular buds is observed after 4 days of angiogenesis induction by corneal suture.[8] The extended time for EPC network formation observed in our study may be explained by the absence of the angiogenic microenvironment stimulated during the inflammatory response caused by corneal suture *in vivo*. Another possible explanation for the delayed onset of EPC network formation found in SS-MNC cocultures in comparison to SMC cocultures could be due to differences in Angiopoietin-1 and Tie-2 signaling, critical for the regulation of pericyte and EC interactions.[2] There may also exist differences in the extracellular matrix composition between SMC and SS-MNC cocultures that could affect subsequent EPC network formation. For example, collagen I can induce EC capillary morphogenesis whereas laminin-1 can suppress EC activation and subsequent microvessel formation.[40] To be thorough, an investigation into the contributions of different ECM components, as well as the role of their corresponding integrin ligands within EPC and SS-MNC coculture systems, should be analyzed in a future study. While further investigations are needed to characterize EPCs as undergoing vasculogenesis, the cocultures of SS-MNCs and EPCs may provide a novel *in vitro* model for investigating *de novo* microvessel formation.

An unexpected finding from our study was the difference in angiogenic potential between mural cell subtypes HVPs and SMCs. While employing HVPs and SMCs as a positive control to evaluate the mural cell potential of SS-MNCs in supporting EPC network formation within a minimalist coculture system, we observed HVPs were not able to support

EPC network formation over 14 days of coculture in contrast SMCs. Although both pericytes and SMCs are included in the class of mural cells[1,3,18] their distinct roles in supporting EPC microvessel formation are not well understood. Previously reported studies demonstrated the ability of HVPs to support angiogenesis of ECs utilized biologically-derived gels[9] or supplemental, angiogenic growth factors.[39] Based on our findings, SMCs are a more angiogenic mural cell than HVPs due to their ability to sustain EPC network formation without additional stimulants provided in the culture media or tissue-culture substrate. Although the SS-MNCs were shown in this study to possess characteristics of both SMC and HVPs, further characterization in defining mural cells is needed before any definitive classifications can be made regarding the identity of SS-MNCs.

Another unanticipated finding from this study was the intriguing formation of 3D microvessel structures upon induction of SS-MNC and EPC cocultures within osteogenic media. These microvascular structures are similar to results found utilizing human fetal bone marrow-derived MSCs in coculture with EPCs.[27] In addition, the networks formed using our SS-MNC conditions were stable for up to 18 days in culture, an improvement over microvasculature formed using fetal-derived MSCs, which regressed by 14 days of culture.[27]

In conclusion, our findings identify an angiogenic population of MNCs that phenotypically resemble pericytes and support the formation of microvascular networks from EPCs. The results of our study strengthen the use of umbilical cord blood as a single tissue source for the isolation of both endothelial and mural progenitor cells to use in microvascular tissue engineering applications.

Supplementary Material

Refer to Web version on PubMed Central for supplementary material.

Acknowledgments

This work was supported in part by NIH Grant HL88825. E.B.P. was supported by a National Science Foundation Graduate Research Fellowship. This work was also supported by the Flight Attendant Medical Research Institute (Young Clinical Scientist Award to N.C.).

References

1. Adams RH, Alitalo K. Molecular regulation of angiogenesis and lymphangoigenesis. Nat Rev. 2007; 8:464–478.
2. Armulik A, Abramsson A, Betsholtz C. Endothelial/pericyte interactions. Circ Res. 2005; 97:512–523. [PubMed: 16166562]
3. Armulik A, Genové G, Betsholtz C. Pericytes: developmental, physiological, and pathological perspectives, problems, and promises. Dev Cell. 2011; 21:193–215. [PubMed: 21839917]
4. Attar A, Ghalyanchi Langeroudi A, Vassaghi A, Ahrari I, Maharlooei MK, Monabati A. Role of CD271 enrichment in the isolation of mesenchymal stromal cells from umbilical cord blood. Cell Biol Int. 2013; 37:1010–1015. [PubMed: 23619775]
5. Bhang SH, Lee S, Shin JY, Lee TJ, Kim BS. Transplantation of cord blood mesenchymal stem cells as spheroids enhances vascularization. Tissue Eng Part A. 2012; 18:2138–2147. [PubMed: 22559333]

6. Birbrair A, Zhang T, Wang ZM, Messi ML, Mintz A, Delbono O. Type-1 pericytes participate in fibrous tissue deposition in aged skeletal muscle. Am J Physiol Cell Physiol. 2013; 305:C1098–C1113. [PubMed: 24067916]
7. Blocki A, Wang Y, Koch M, Peh P, Beyer S, Law P, Hui J, Raghunath M. Not all MSCs can act as pericytes: functional in vitro assays to distinguish pericytes from other mesenchymal stem cells in angiogenesis. Stem Cells Dev. 2013; 22:2347–2355. [PubMed: 23600480]
8. Bourghardt Peebo B, Fagerholm P, Traneus-Röckert C, Lagali N. Time-lapse in vivo imaging of corneal angiogenesis: the role of inflammatory cells in capillary sprouting. Invest Ophthalmol Vis Sci. 2011; 10:3060–3068. [PubMed: 21330652]
9. Butler JM, Kobayashi H, Rafii S. Instructive role of the vascular niche in promoting tumour growth and tissue repair by angiogenic factors. Nat Rev Cancer. 2010; 10:138–146. [PubMed: 20094048]
10. Caplan AI. All MSCs are pericytes? Cell Stem Cell. 2008; 3:229–230. [PubMed: 18786406]
11. Chen WC, Park TS, Murray IR, Zimmerlin L, Lazzari L, Huard J, Péault B. Cellular kinetics of perivascular MSC precursors. Stem Cells Int. 2013; 2013:983059. [PubMed: 24023546]
12. Covas DT, Panepucci RA, Fontes AM, Jr WA, Orellana Silva MD, Freitas MC, Neder L, Santos AR, Peres LC, Jamur MC, Zago MA. Multipotent mesenchymal stromal cells obtained from diverse human tissues share functional properties and gene-expression profile with CD146+ perivascular cells and fibroblasts. Exp Hematol. 2008; 36:642–654. [PubMed: 18295964]
13. Crisostomo PR, Wang M, Wairiuko GM, Morrell ED, Terrell AM, Seshadri P, Nam UH, Meldrum DR. High passage number of stem cells adversely affects stem cell activation and myocardial protection. Shock. 2006; 26:575–580. [PubMed: 17117132]
14. Dominici M, Le Blanc K, Mueller I, Slaper-Cortenbach I, Marini F, Krause D, Deans R, Keating A, Prockop DJ, Horwitz E. Minimal criteria for defining multipotent mesenchymal stromal cells. The international society for cellular therapy position statement. Cytotherapy. 2006; 8:315–317. [PubMed: 16923606]
15. Evensen L, Micklem DR, Blois A, Berge SV, Aarsaether N, Littlewood-Evans A, Wood J, Lorens JB. Mural cell associated VEGF is required for organotypic vessel formation. PLoS One. 2009; 4:e5798. [PubMed: 19495422]
16. Ferrara N, Kerbel RS. Angiogenesis as a therapeutic target. Nature. 2005; 438:967–974. [PubMed: 16355214]
17. Foo SS, Turner CJ, Adams S, Compagni A, Aubyn D, Kogata N, Lindblom P, Shani M, Zicha D, Adams RH. Ephrin-B2 controls cell motility and adhesion during blood-vessel-wall assembly. Cell. 2006; 124:161–173. [PubMed: 16413489]
18. Herbert SP, Stainier DY. Molecular control of endothelial cell behavior during blood vessel morphogenesis. Nat Rev Mol Cell Biol. 2011; 12:551–564. [PubMed: 21860391]
19. Hirschi KK, Ingram DA, Yoder MC. Assessing identity, phenotype, and fate of endothelial progenitor cells. Arterioscler Thromb Vasc Biol. 2008; 28:1584–1595. [PubMed: 18669889]
20. Hirvonen T, Suila H, Tiitinen S, Natunen S, Laukkanen ML, Kotovuori A, Reinman M, Satomaa T, Alfthan K, Laitinen S, Takkinen K, Räbinä J, Valmu L. Production of a recombinant antibody specific for I blood group antigen, a mesenchymal stem cell marker. Bioresour Open Access. 2013; 2:336–345.
21. Ingram DA, Mead LE, Tanaka H, Meade V, Fenoglio A, Mortell K, Pollok K, Ferkowicz MJ, Gilley D, Yoder MC. Identification of a novel hierarchy of endothelial progenitor cells using human peripheral and umbilical cord blood. Blood. 2004; 104:2752–2760. [PubMed: 15226175]
22. Kleinman HK, McGarvey ML, Liotta LA, Robey PG, Tryggvason K, Martin GR. Isolation and characterization of type IV procollagen, laminin, and heparan sulfate proteoglycan from the EHS sarcoma. Biochemistry. 1982; 21:6188–6193. [PubMed: 6217835]
23. Korff T, Kimmina S, Martiny-Baron G, Augustin HG. Blood vessel maturation in a 3-dimensional spheroidal coculture model: direct contact with smooth muscle cells regulates endothelial cell quiescence and abrogates VEGF responsiveness. FASEB J. 2001; 15:447–457. [PubMed: 11156960]
24. Kretlow JD, Jin YQ, Liu W, Zhang WJ, Hong TH, Zhou G, Baggett LS, Mikos AG, Cao Y. Donor age and cell passage affects differentiation potential of murine bone marrow-derived stem cells. BMC Cell Biol. 2008; 9:60. [PubMed: 18957087]

25. Laitinen A, Nystedt J, Laitinen S. The isolation and culture of human cord blood-derived mesenchymal stem cells under low oxygen conditions. Methods Mol Biol. 2011; 698:63–73. [PubMed: 21431511]
26. Lee OK, Kuo TK, Chen WM, Lee KD, Hsieh SL, Chen TH. Isolation of multipotent mesenchymal stem cells from umbilical cord blood. Blood. 2004; 103:1669–1675. [PubMed: 14576065]
27. Liu Y, Teoh SH, Chong MS, Yeow CH, Kamm RD, Choolani M, Chan JK. Contrasting effects of vasculogenic induction upon biaxial bioreactor stimulation of mesenchymal stem cells and endothelial progenitor cells cocultures in three-dimensional scaffolds under in vitro and in vivo paradigms for vascularized bone tissue engineering. Tissue Eng Part A. 2013; 19:893–904. [PubMed: 23102089]
28. Markov V, Kusumi K, Tadesse MG, William DA, Hall DM, Lounev V, Carlton A, Leonard J, Cohen RI, Rappaport EF, Saitta B. Identification of cord blood-derived mesenchymal stem/stromal cell populations with distinct growth kinetics, differentiation potentials, and gene expression profiles. Stem Cells Dev. 2007; 16:53–73. [PubMed: 17348805]
29. Medici D, Kalluri R. Endothelial-mesenchymal transition and its contribution to the emergence of stem cell phenotype. Semin Cancer Biol. 2012; 22:379–384. [PubMed: 22554794]
30. Medici D, Shore EM, Lounev VY, Kaplan FS, Kalluri R, Olsen BR. Conversion of vascular endothelial cells into multipotent stem-like cells. Nat Med. 2010; 16:1400–1406. [PubMed: 21102460]
31. Melero-Martin JM, De Obaldia ME, Kang SY, Khan ZA, Yuan L, Oettgen P, Bischoff J. Engineering robust and functional vascular networks in vivo with human adult and cord blood derived progenitor cells. Circ Res. 2008; 103:194–202. [PubMed: 18556575]
32. Melero-Martin JM, Khan ZA, Picard A, Wu X, Paruchuri S, Bischoff J. In vivo vasculogenic potential of human blood-derived endothelial progenitor cells. Blood. 2007; 109:4761–4768. [PubMed: 17327403]
33. Moonen JR, Krenning G, Brinker MG, Koerts JA, van Luyn MJ, Harmsen MC. Endothelial progenitor cells give rise to pro-angiogenic smooth muscle-like progeny. Cardiovasc Res. 2010; 86:506–515. [PubMed: 20083576]
34. Novosel EC, Kleinhans C, Kluger PJ. Vascularization is the key challenge in tissue engineering. Adv Drug Deliv Rev. 2011; 63:300–311. [PubMed: 21396416]
35. Orr AW, Elzie CA, Kucik DF, Murphy-Ullrich JE. Thrombospondin signaling through the calreticulin/LDL receptor-related protein co-complex stimulates random and directed cell migration. J Cell Sci. 2003; 116:2917–2927. [PubMed: 12808019]
36. Pedersen TO, Blois AL, Xue Y, Xing Z, Cottler-Fox M, Fristad I, Leknes KN, Lorens JB, Mustafa K. Osteogenic stimulatory conditions enhance growth and maturation of endothelial cell microvascular networks in culture with mesenchymal stem cells. J Tissue Eng. 2012; 3:2041731412443236. [PubMed: 22511994]
37. Peters EB, Christoforou N, Leong KW, Truskey GA. Comparison of mixed and lamellar coculture spatial arrangements for tissue engineering capillary networks in vitro. Tissue Eng Part A. 2013; 19:697–706. [PubMed: 23171167]
38. Roura S, Bagó JR, Soler-Botija C, Pujal JM, Gálvez-Montón C, Prat-Vidal C, Llucià-Valldeperas A, Blanco J, Bayes-Genis A. Human umbilical cord blood-derived mesenchymal stem cells promote vascular growth in vivo. PLoS One. 2012; 7:e49447. [PubMed: 23166670]
39. Saik JE, Gould DJ, Keswani AH, Dickinson ME, West JL. Biomimetic hydrogels with immobilized ephrinA1 for therapeutic angiogenesis. Biomacromolecules. 2011; 12:2715–2722. [PubMed: 21639150]
40. Senger DR, Davis GE. Angiogenesis. Cold Spring Harb Perspect Biol. 2011; 3:a005090. [PubMed: 21807843]
41. Sharma RR, Pollock K, Hubel A. Mesenchymal stem or stromal cells: a review of clinical applications and manufacturing practices. Transfusion. 2014; 54:1418–1437. [PubMed: 24898458]
42. Stanevsky A, Goldstein G, Nagler A. Umbilical cord blood transplantation: pros, cons and beyond. Blood Rev. 2009; 23:199–204. [PubMed: 19282073]
43. ten Dijke P, Arthur HM. Extracellular control of TGFbeta signaling in vascular development and disease. Nat Rev Mol Cell Biol. 2007; 8:857–869. [PubMed: 17895899]

44. Wagner W, Bork S, Horn P, Krunic D, Walenda T, Diehlmann A, Benes V, Blake J, Huber FX, Eckstein V, Boukamp P, Ho AD. Aging and replicative senescence have related effects on human stem and progenitor cells. PLoS One. 2009; 4:e5846. [PubMed: 19513108]
45. Yee D, Hanjaya-Putra D, Bose V, Luong E, Gerecht S. Hyaluronic acid hydrogels support cord-like structures from endothelial colony-forming cells. Tissue Eng Part A. 2011; 17:1351–1361. [PubMed: 21247340]
46. Zarem HA. The microcirculatory events within full-thickness skin allografts (homo-grafts) in mice. Surgery. 1969; 66:392–397. [PubMed: 4894474]
47. Zhang X, Hirai M, Cantero S, Ciubotariu R, Dobrila L, Hirsh A, Igura K, Satoh H, Yokomi I, Nishimura T, Yamaguchi S, Yoshimura K, Rubinstein P, Takahashi TA. Isolation and characterization of mesenchymal stem cells from human umbilical cord blood: reevaluation of critical factors for successful isolation and high ability to proliferate and differentiate to chondrocytes as compared to mesenchymal stem cells from bone marrow and adipose tissue. J Cell Biochem. 2011; 112:1206–1218. [PubMed: 21312238]

Abbreviations

EC	Endothelial cell
EndMT	Endothelial-to-mesenchymal transition method for isolating MPCs from cord blood
EPC	Endothelial progenitor cell
HUVEC	Human umbilical vein-derived endothelial cell
HVP	Human vascular pericyte
MNC	Mononuclear cell
MPC	Mesenchymal progenitor cell
MSC	Mesenchymal stem cell
SMC	Smooth muscle cell
SS-MNC	Spindle-shaped mononuclear cell
TM	Traditional method for isolating MPCs from cord blood

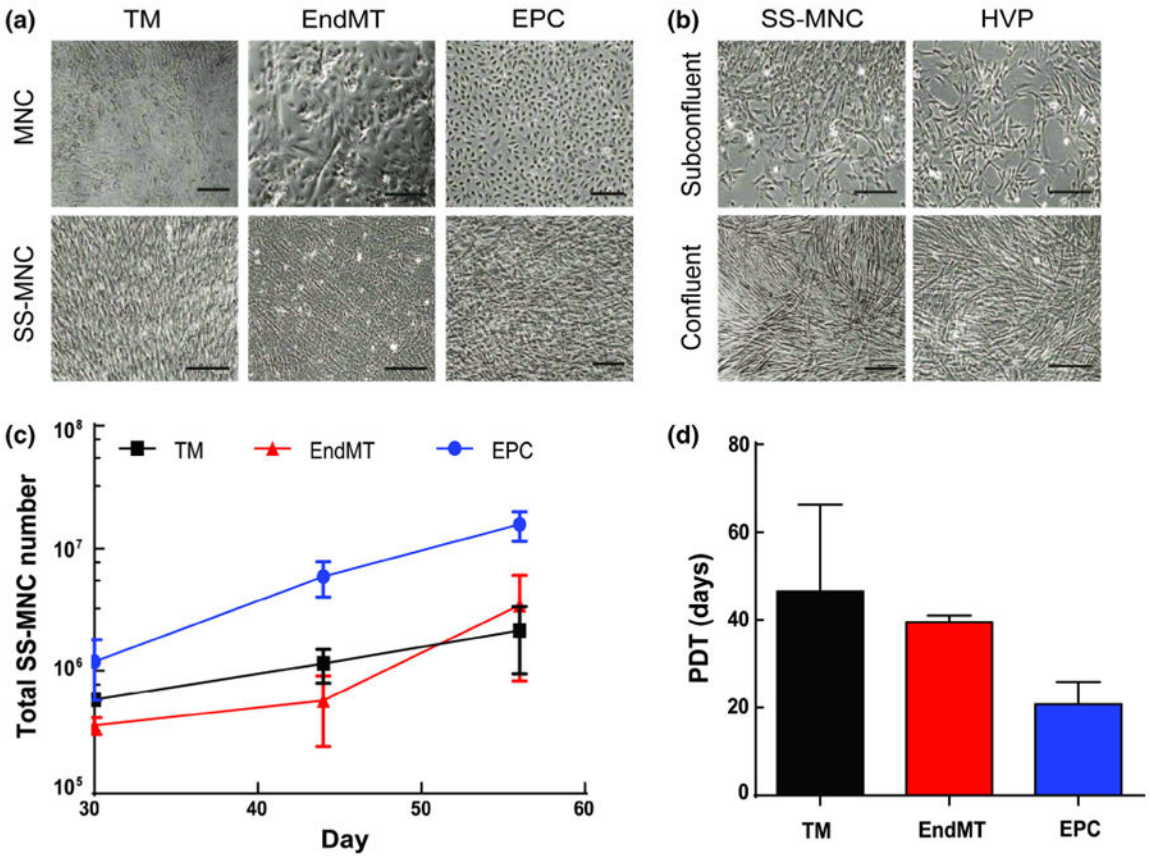

Figure 1.

Comparison of isolation methods for obtaining pericyte-like cells from umbilical cord blood. (a) Mononuclear cells (MNCs) resulting from traditional (TM), endothelial-to-mesenchymal transition (EndMT), and endothelial progenitor cell (EPC) isolation methods. A subpopulation of spindle-shaped MNCs (SS-MNCs) were observed in all isolation methods; (b) Comparison of the morphology of SS-MNCs, derived using EPC isolation methods, with human vascular pericytes (HVPs) at subconfluent and confluent densities. Scale bars equal 200 μm; (c) The expansion potential of SS-MNCs derived from EPC (n = 3), TM (n = 2), and EndMT (n = 2) isolation methods were assessed during the first 60 days in culture. (d) Population doubling time (PDT) for SS-MNCs derived using TM, EndMT, and EPC isolation methods during the first 45 days of culture. Error bars in panels (d) and (e) indicate standard deviation.

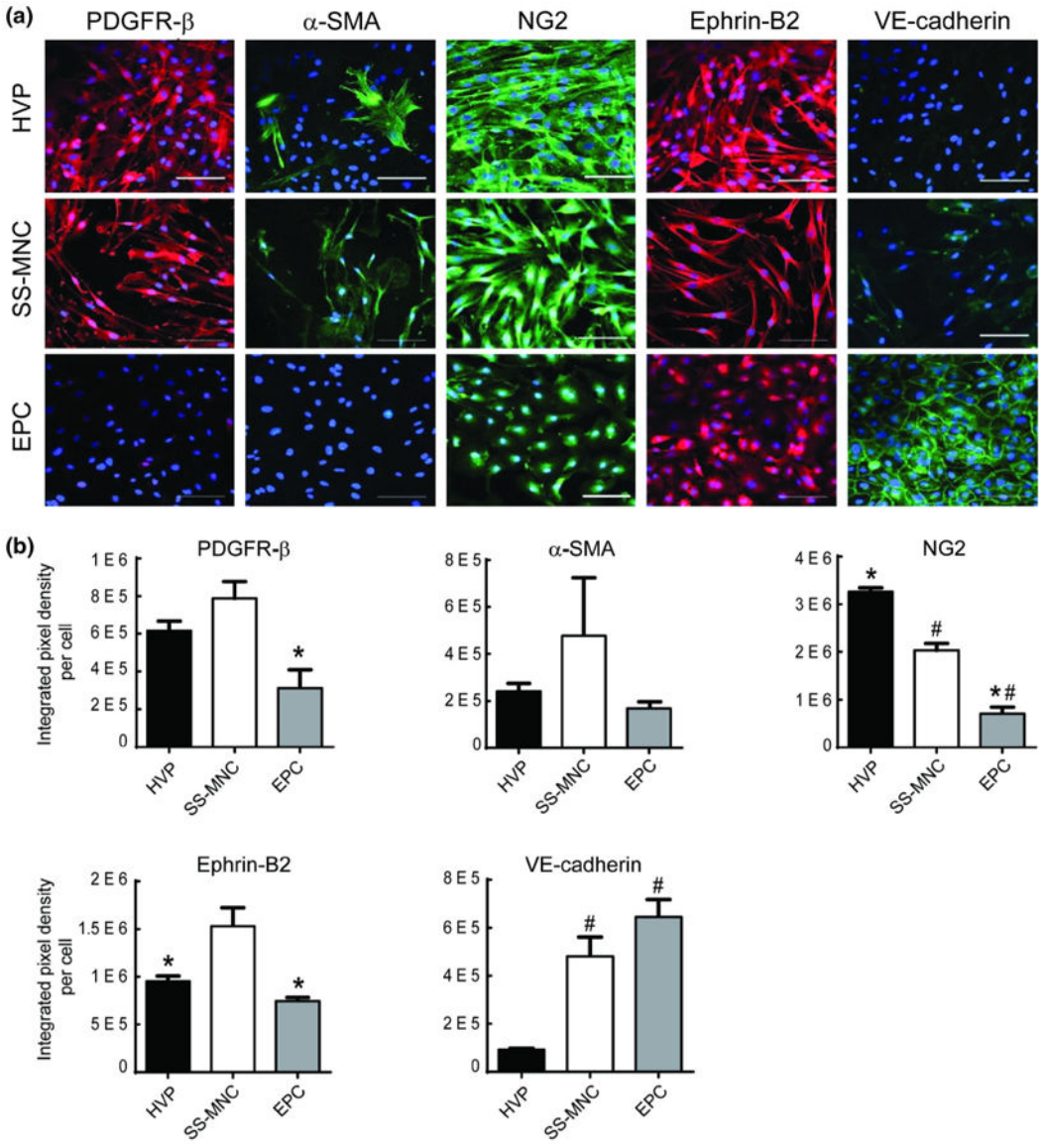

Figure 2.

Evaluation of SS-MNCs for pericyte phenotype. (a) Representative immunofluorescence images comparing expression of pericyte-associated markers PDGFR-*β*, *α*-SMA, NG2, and ephrin-B2 and endothelial cell marker (VE-cadherin) between HVPs, SS-MNCs, and EPCs. Nuclei were counterstained with DAPI (blue). Scale bar equals 100 *μ*m. (b) Quantitative comparison of immunofluorescence expression for PDGFR-*β*, *α*-SMA, NG2, ephrin-B2, and VE-cadherin between HVPs, SS-MNCs, and EPCs assessed by integrated pixel density per cell. **p*<0.05 in comparison to SS-MNCs, $^{\#}p$<0.05 in comparison to HVPs. Error bars indicate standard error of the mean. *n* = 3 images analyzed per condition. Image area analyzed is 0.15 mm^2.

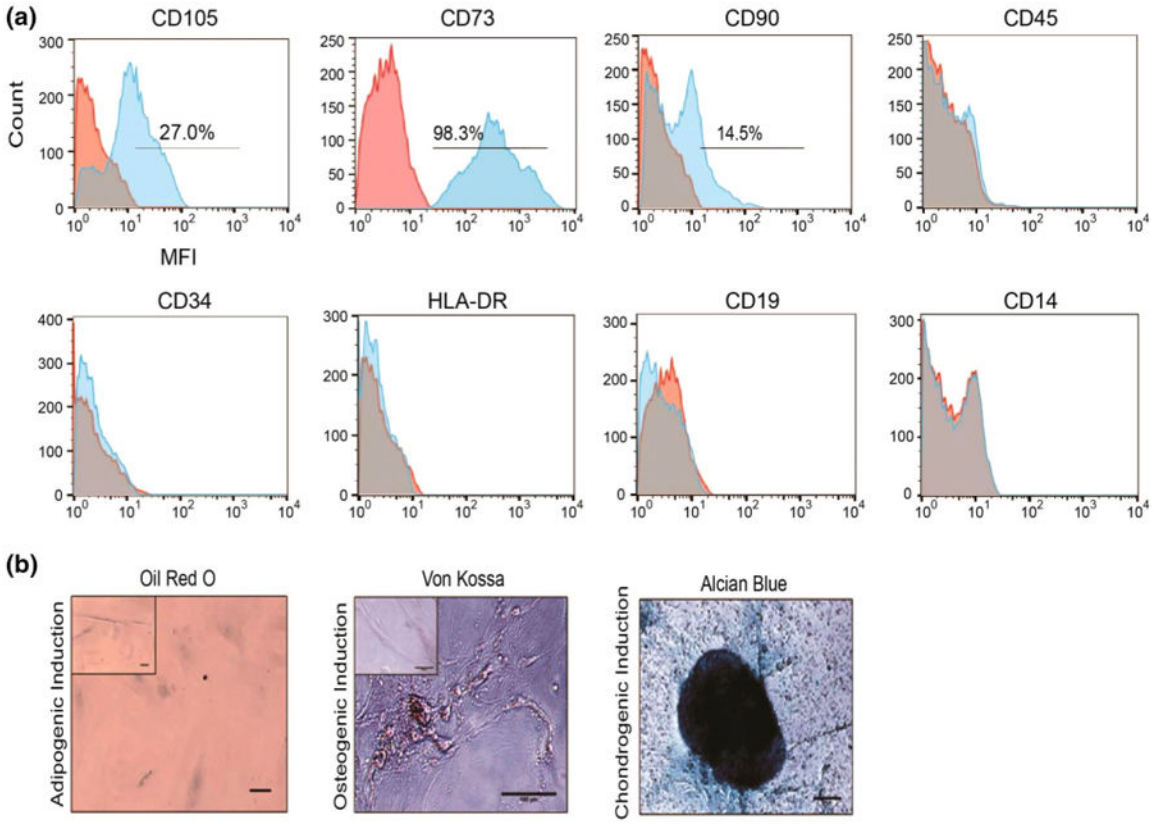

Figure 3.

Evaluation of SS-MNCs for mesenchymal stem cell phenotype and function. (a) Representative histograms depicting SS-MNC surface marker expression though median fluorescence intensity (MFI) for CD105, CD73, CD90, CD45, CD34, HLA-DR, CD19, CD14 in comparison to mouse IgG isotype control. (b) Representative images of SS-MNCs after culture with induction media towards adipogenic, osteogenic, or chondrogenic lineage and staining with Oil Red O, von Kossa, or Alcian blue, respectively. Insets represent control conditions. Scale bar equals 100 μm.

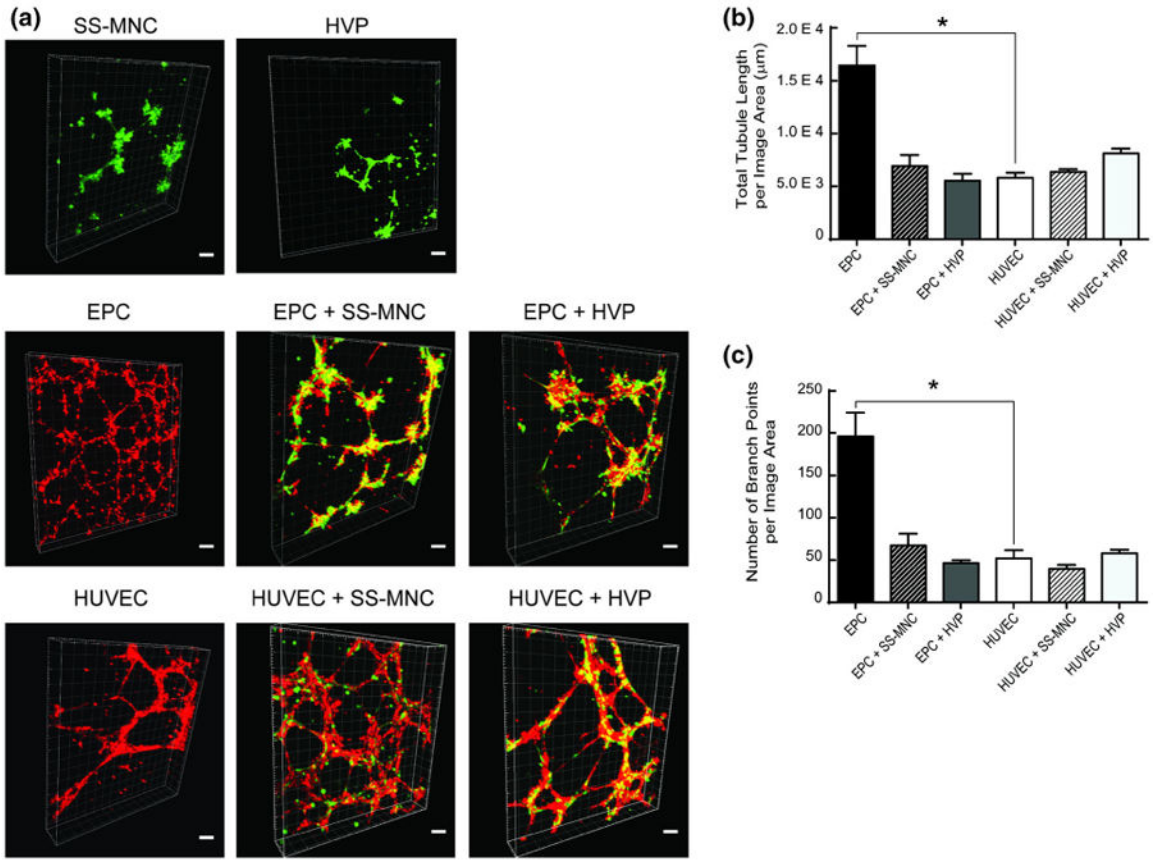

Figure 4.

Evaluation of SS-MNCs for angiogenic pericyte function within a Matrigel™ system. (a) Representative images of network formation from 3 independent experiments between monocultures and cocultures of SS-MNCs, HVPs, HUVECs, and EPCs upon Matrigel™ 6 h after plating. To visualize networks and interactions between cell types, HUVECs and EPCs were transduced with tdTomato lentivirus and SS-MNCs and HVPs transduced with GFP. Images are 3D projections from a 200-um thick z-stack, taken at 10 μm intervals. Scale bar equals 100 μm. (b, c) Quantification of network morphology for total tubule length and branch points was performed over an image area of 2.4 mm^2. n = 4 images analyzed per condition, *p<0.0001.

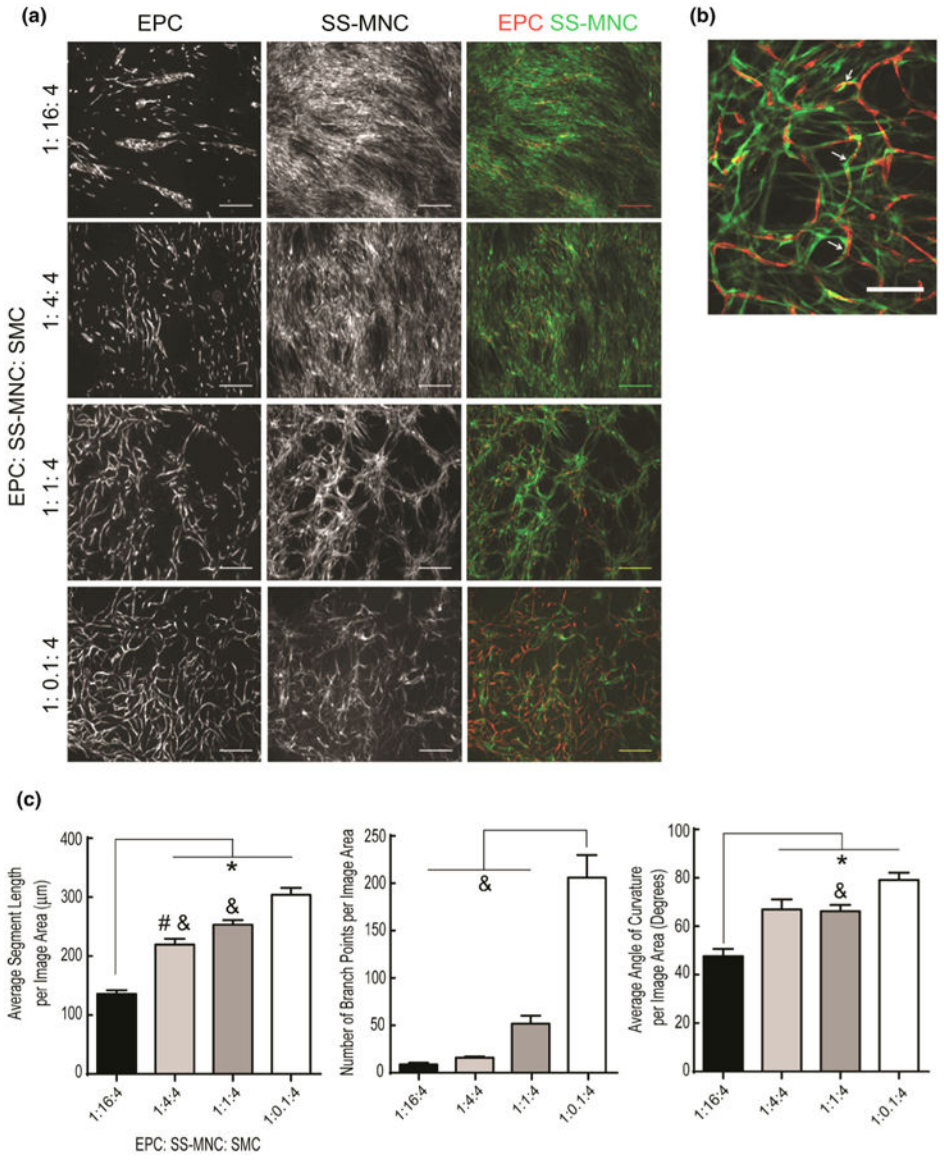

Figure 5.

Evaluation of SS-MNC on EPC network formation when placed in tri-culture with angiogenic mural cells. (a) Representative images at day 9 of culture depicting EPCs, transduced with tdTomato lentivirus, and SS-MNCs, transduced with GFP lentivirus. SMCs are unlabeled.The ratio of SS-MNCs to SMCs was varied while the number of EPCs remained constant.Scale bar equals 500 μm. (b) Enlarged representative image depicting intimate pericyte-like association of SS-MNCs (green) to EPCs (red) at a 1:1:4 ratio of EPCs to SS-MNCs to SMCs. Scale bar equals 200 μm. (c) Quantification of average segment length, number of branch points, and angle of curvature for microvessel networks as a function of EPC:SS-MNC:SMC ratio in triculture experiments. Image area analyzed is 7 mm^2. n = 4 images analyzed per condition. *statistical significance (p<0.05) against the 1:16:4 ratio, ^statistical significance against the 1:4:4 ratio, #statistical significance against the 1:1:4 ratio, &statistical significance against the 1:0.1:4 ratio.

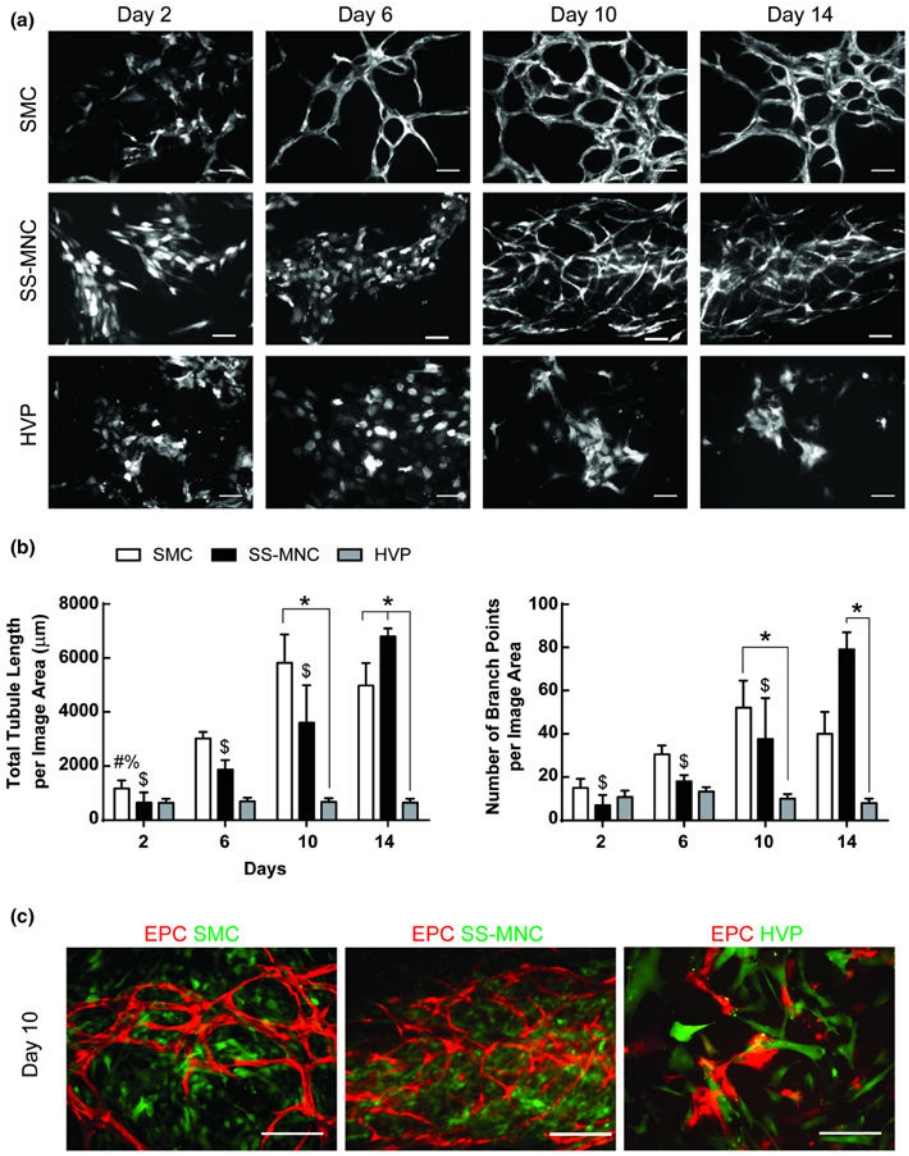

Figure 6.

Evaluation of the angiogenic, mural cell function of SS-MNCs through support of EPC network formation. (a) Representative images of EPCs transduced with tdTomato lentivirus in coculture with SMCs, SS-MNCs, or HVPs over 14 days of culture. Scale bar equals 100 μm. (b) Quantification of EPC networks for total tubule length and number of branch points. *$p<0.05$, $^{\#}p<0.05$ in comparison to day 10 of SMC coculture, $^{\%}p<0.05$ in comparison to day 14 of SMC coculture, $^{\$}p<0.05$ in comparison to day 14 of SS-MNC coculture. Image area analyzed equals 0.57 mm^2. (c) Overlay images of SMCs, SS-MNCs, or HVPs (green) at day 10 of coculture with EPCs (red). Scale bar equals 200 μm.

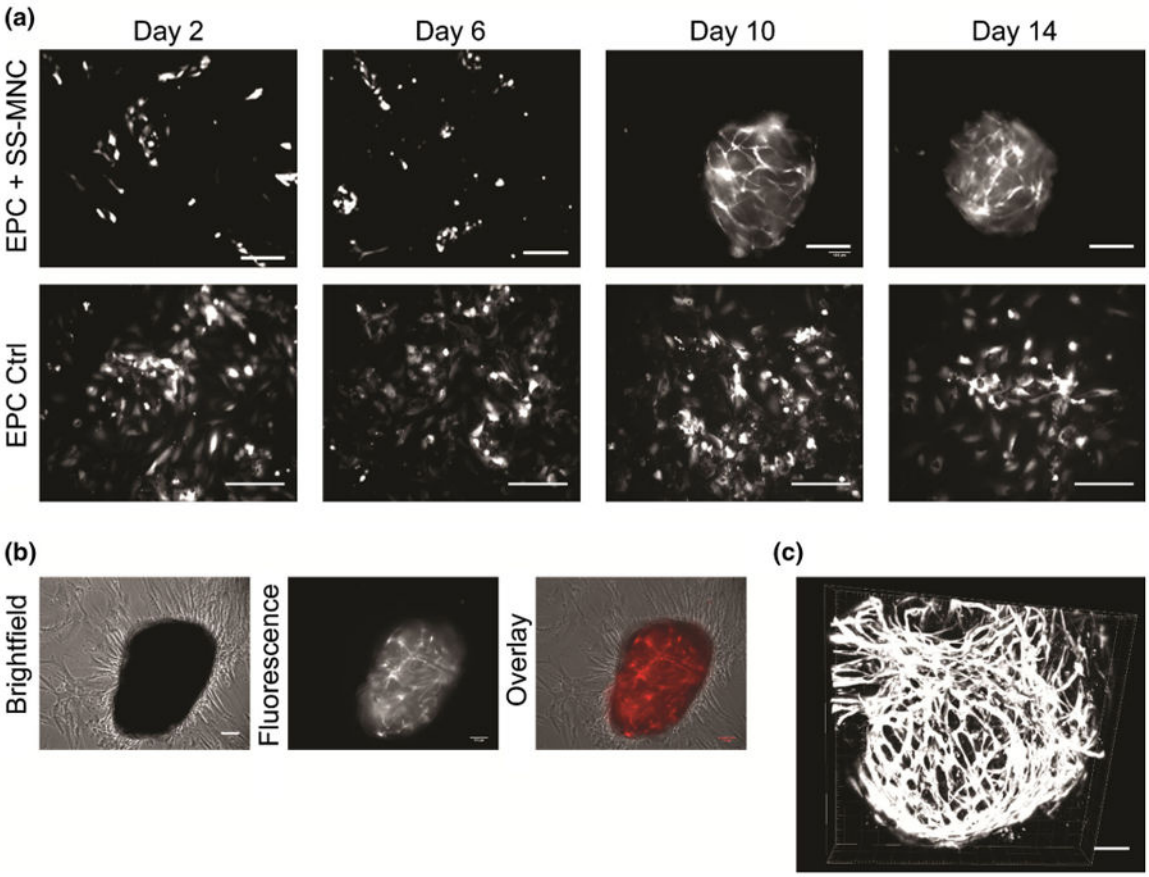

Figure 7.

Evaluation of osteogenic media conditions to enhance the ability of SS-MNCs to support EPC network formation *in vitro*. (a) Representative images of EPCs transduced with tdTomato lentivirus, in monoculture or coculture with SS-MNCs within osteogenic media conditions during the first 14 days of culture. Scale bar equals 200 μm. (b) Brightfield and fluorescent overlay depicting 3D nodule formation of tdTomato-transduced EPCs in coculture with SS-MNCs at day 10 of osteogenic media coculture. Scale bar equals 100 μm. (c) 3D EPC microvessel structures after 10 days of coculture with SS-MNCs containing osteogenic media. Scale bar equals 100 μm. Image depth equals 75 μm.

Table 1

Primer sequences for evaluating EPC and MPC identity of MNCs.

Gene	Forward primer	Reverse primer
PECAM-1	5′-TGA GTC TAG GTC GGGGAG TG-3′	5′-GAG CAT ATA CTG GTCGCC CC-3′
α-SMA	5′-AGC GAC CCT AAA GCTTCC CA-3′	5′-CAT AGA GAG ACA GCACCG CC-3′
VE-Cadherin	5′-CGG CTA GGC ATA GCATTG GA-3′	5′-TGT TGG CCG TGT TATCGT GA-3′
FSP-1	5′-GGT GAA GAA GAT GGGTGG GG-3′	5′-CTG CAG CCA CCT GGTCTA TT′-3′
18s rRNA	5′-CCG CTT TCT GCC GAGATG CC-3′	5′-GCT GCC CAA TCC CCGTGT TG-3′